Synthesis of Copper Nanowires via a Complex-Surfactant-Assisted Hydrothermal Reduction Process

ARTICLE *in* THE JOURNAL OF PHYSICAL CHEMISTRY B · OCTOBER 2003

Impact Factor: 3.3 · DOI: 10.1021/jp036023s

Synthesis of Copper Nanowires via a Complex-Surfactant-Assisted Hydrothermal Reduction Process

Zhaoping Liu,[†] You Yang,[†] Jianbo Liang,[†] Zhaokang Hu,[†] Shu Li,[†] Sheng Peng,[†] and Yitai Qian*[,†,‡]

Structure Research Laboratory and Department of Chemistry, University of Science and Technology of China, Hefei, Anhui 230026, P. R. China

Received: July 14, 2003; In Final Form: September 16, 2003

This paper describes a simple complex-surfactant-assisted hydrothermal reduction approach to the facile synthesis of metal copper nanowires with average diameters of ∼85 nm and lengths of several tens of micrometers. These copper nanowires were formed through the reduction of the Cu^{II}−glycerol complexes ($Cu(C_3H_6O_3)$) by phosphite (HPO_3^{2-}) in the presence of surfactant sodium dodecyl benzenesulfonate (SDBS) at 120 °C. High-resolution transmission electron microscopy (HRTEM) and selected-area electron diffraction (SAED) indicate that the resulted nanowires had preferred [1$\bar{1}$0] growth direction. The formation mechanism for Cu nanowires had been properly proposed. Some influencing factors on the morphologies of the final products had also been discussed.

Introduction

One-dimensional (1D) nanostructures of metals are expected to play an important role in fabricating nanoscale electronic, optoelectronic, and magnetic devices, which also provide an ideal model system to experimentally investigate physical phenomena such as quantized conductance and size effects.[1] Among all metals, copper is the most commonly used as an interconnect due to its high electrical conductivity. The availability of copper nanowires with well-defined dimensions should be able to bring in new types of applications or enhance the performance of currently existing electric devices as a result of quantum-size effects.[2] Up to now, the fabrication of copper nanowires is mainly achieved by template-directed methods involving electrochemical deposition and the reduction of copper compounds in the channels of the template.[3] Although these templates were effective in preparing nanowires with uniform and controllable dimensions, they usually lead to complicated processes and they also needed to be removed to obtain the individual nanowires, while the yield is relatively low. Recently, some templateless approaches, such as vacuum vapor deposition (VVD) and vapor−solid reaction growth (VSRG), have also been developed to fabricate copper nanowires.[4] But they are often based on special instruments or harsh conditions. Although the formation of nanowires of many materials has been achieved by a solution-phase method,[5] the growth of metal (such as Cu) nanowires from isotropic solutions has been a more challenging task due to its highly symmetric cubic lattices. More recently, some face-centered cubic metal (such as Ag and Pb) nanowires have been successfully achieved by a solution-phase route.[6] This reminded us that Cu nanowires might be synthesized by a rational solution-phase route.

Herein, a surfactant-assisted hydrothermal reduction process was developed to synthesize copper nanowires with high yield. Such a process involved the nucleation of copper nanoparticles through the reduction of the complex Cu^{II}−glycerol by HPO_3^{2-} in a high concentration of NaOH and glycerol aqueous solutions and then the growth of copper nanowires with the assistance of a suitable surfactant, sodium dodecyl benzenesulfonate (SDBS). The redox reaction can be expressed as

$$Cu(C_3H_6O_3) + HPO_3^{2-} + OH^- = Cu + C_3H_8O_3 + PO_4^{3-}$$

Experimental Section

All of the chemical regents used in this experiment were analytical grade. In a typical procedure, $CuSO_4 \cdot 5H_2O$, glycerol, NaOH, H_3PO_3, and SDBS were introduced into distilled water to give a dark-blue solution containing 50 mM Cu^{II}−glycerol complexes, 40 vol % glycerol, 5 M NaOH, 200 mM Na_2HPO_3, and 3 mM SDBS. Then 45 mL of the mixture solution was transferred into a Teflon-lined autoclave of 55 mL capacity. The autoclave was maintained at 120 °C for 20 h and then cooled to room temperature naturally. The resulting red fluffy solid product was filtered and washed, and finally dried in a vacuum at 60 °C for 4 h.

The X-ray diffraction (XRD) analysis was performed using a Rigaku (Japan) D/max-γA X-ray diffractionmeter equipped with graphite monochromatized Cu Kα radiation (λ = 1.54178 Å). The X-ray photoelectron spectra (XPS) were collected on an ESCALab MKII X-ray photoelectron spectrometer, using nonmonochromatized Mg Kα X-ray as the excitation source. The SEM images were taken on a field emission scanning electron microscope (JEOL JSM-6300F, 15 kV). The TEM images were recorded on a Hitachi 800 transmission electron microscopy (TEM) performed at 200 kV. The HRTEM images and the corresponding selected-area electron diffraction (SAED) patterns were taken on a JEOL 2010 high-resolution transmission electron microscope performed at an acceleration voltage of 200 kV. The absorption spectrum was recorded on a UV−vis spectrophotometer (Shimadzu UV-240) in the wavelength range of 500−700 nm.

* To whom correspondence should be addressed. E-mail: ytqian@ustc.edu.cn. Fax: +86-551-3607402. Phone: +86-551-3603204.
[†] Department of Chemistry.
[‡] Structure Research Laboratory.

10.1021/jp036023s CCC: $25.00
Published on Web 10/25/2003

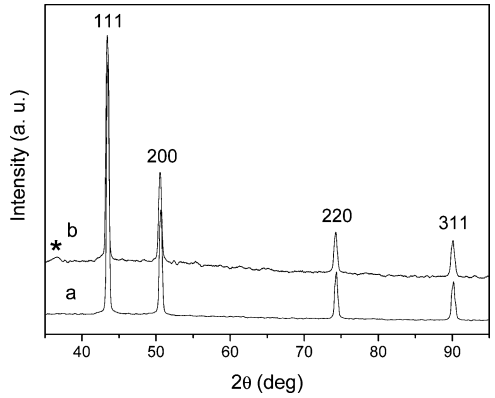

Figure 1. XRD pattern of the products: (a) a fresh sample; (b) a sample that were exposed in atmosphere for 24 h.

Results and Discussion

Phase and Purity of the Products. The phase and purity of the as-obtained products was determined from the XRD pattern shown in Figure 1a. All the peaks can be indexed as face-centered cubic copper with lattice constant $a = 3.614$ Å, which is very close to the reported data (JCPDS 4-836, $a = 3.615$ Å). No characteristic peaks of impurities of oxides can be detected. This indicated that metal copper products were obtained under current synthetic conditions. Because metal copper can be slowly oxidized into Cu_2O and final CuO in the atmosphere, the products should be surface-oxidized inevitably, and the compositions of the oxides layers depend on the periods of exposure time. The XRD pattern of a sample after being exposed for 24 h is shown in Figure 1b, in which a new peak appears with very weak intensity. Judged from the peak position, the weak peak can be appropriately indexed as 111 diffraction of a cubic structure of Cu_2O (cuprite) (JCPDS 5-667). This means the samples used for some measurements (in particular, TEM and SEM) were usually surface-oxidized.

The surface information of the same sample as shown in Figure 1b can be properly provided by XPS. The binding energies obtained in XPS analysis were corrected with the reference to C_{1s} (284.6 eV). The core-level spectrum of Cu 2p (Figure 2a) illustrates that the observed value of the binding energy for Cu $2p_{3/2}$ (932.2 eV) is in good agreement with data observed for Cu^0 or Cu^+.[7] The kinetic energy of the Cu LVV peak is 916.8 eV (Figure 2b). Therefore the value of the "modified Auger parameter" is 1849 eV, which indicates that the existence of Cu^+ besides Cu^0.[8] Additionally, the Cu $2p_{3/2}$ satellite peaks characterizing Cu^{2+},[9] which centered at about 944 eV, are also found in Figure 2a. However, the main O 1s peak is located at 530.8 eV (Figure 2c). Because the binding energies of O 1s for Cu_2O and CuO are 530.4 and 529.6 eV, respectively,[10] the composition of the oxides layers can be determined to be mainly Cu_2O phase, in good agreement with the result from XRD.

Morphology and Structure Characterization of the Products. The morphology and dimension of the as-prepared products were examined by FESEM. The FESEM images (Figure 3a,b) demonstrate that the final products consist of a large quantity of nanowires with a uniform diameter of about 85 nm and a typical length of several tens of micrometers. These images demonstrate the Cu nanowires could be easily produced in large-scale using the present method.

The structure characterization of individual nanowires was investigated in detail by HRTEM and SAED. The HRTEM image (Figure 4a) of the nanowires clearly demonstrates that the as-obtained Cu nanowires are coated with oxide layers, which are usually 1−2 nm thick. The two set of regular lattice spacings of ca. 0.21 nm (in region A) and ca. 0.30 nm (in region B) correspond to the separation between two $(1\bar{1}1)$ planes of face-centered cubic copper and $(1\bar{1}0)$ planes of cubic Cu_2O (cuprite), respectively. This indicates that the as-synthesized Cu nanowires were single crystalline. The corresponding SAED pattern along the [110] zone axis direction is shown in Figure 4b. Both the SAED pattern and the HRTEM image reveal that the growth plane of the copper nanowires is one of $\{1\bar{1}1\}$ planes and they grow along the $[1\bar{1}0]$ direction. In this SAED pattern, the additional diffraction spots along three directions (including $[1\bar{1}\bar{1}]$, $[1\bar{1}1]$ and $[1\bar{1}0]$) can also be observed. These diffraction spots are not consistent with the previously observed results about the Cu nanrods with 5-fold axis along the [110] direction,[11] implying the structure of the present Cu nanowires seems to differ from the previous report for Cu nanorods, whereas these additional diffraction spots suggest the presence of a presently unknown 7 times superlatice in the three directions. This interesting superlattice may be caused by electron-beam-induced damage (see the Supporting Information). These "large" structures can also be clearly observed in the HRTEM image (Figure 4c).

It has been well understood that the Cu(110) and Cu(001) surfaces show a strong tendency to reconstruct under the chemisorption of oxygen, and a surface models, "missing row" models, has been proposed and confirmed with different techniques, such as low-energy electron-diffraction (LEED), scanning tunneling microscopy (STM), and so on.[12] The mssing-row-type reconstructed arrangement of the surfaces atoms resulted in the formation of Cu_2O layers on both the Cu(110) and the Cu(001) surfaces. Our SAED pattern reveals that the sidewalls of the as-synthesized Cu nanowires are mainly enveloped with {110} and {001} planes. Thus, it can be believed that {110} and {001} surfaces of Cu nanowires have undergone a missing-row-type reconstruction induced by oxygen chemisorption, and this finally led to the formation of Cu_2O layers on the surfaces of Cu nanowires. This SAED pattern also shows the diffraction spots of Cu_2O phase, agreeing with the observation from HRTEM.

TEM Studies on the Nanowires Growth Process. To investigate the nucleation and growth process of these nanowires, we have systematically studied the samples (taken at various stages of reaction) using TEM. Figure 5 shows TEM images of the samples that were obtained after hydrothermal reaction was proceeded for 3, 10, and 20 h. These images clearly exhibit the evolution of Cu nanostructures from nanoparticles to nanowires over time at 120 °C. After heating for 3 h, the blue color of the mixture disappeared, and a large amount of red solid product was generated, indicating the formation of Cu nanoparticles through the reduction of complex $Cu(C_3H_6O_3)$ by HPO_3^{2-}. Figure 5a shows the initial product mainly consisted of nanoparticles with sizes of 100−200 nm. The SAED pattern shown in the inset of this image confirmed that these nanoparticles were of single crystals of face-centered cubic Cu. After 10 h, the products consisted of three different forms of Cu nanostructures, wires (∼40%), rods (∼40%), and particles (∼20%) (see Figure 5b), indicating many nanopaticles had developed into 1D nanostructures of Cu. These 1D nanostructures were ∼80 nm in lateral dimensions. The inset of Figure 5b shows a magnified view of the roots of several nanowires. This image distinctly demonstrates that the Cu nanowires were grown out from the surfaces of seeding nanocrystals. This growth mode was very similar to that most recently reported for Pb nanowires.[6c] It could be believed, therefore, that the formation of Cu nanowires also followed the Ostwald ripening

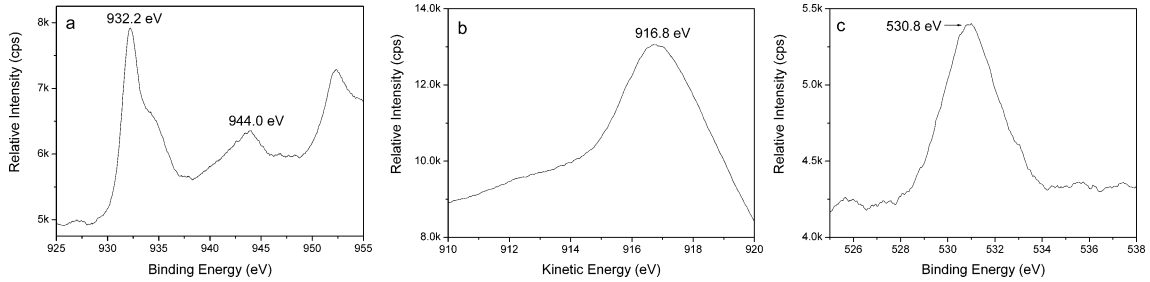

Figure 2. XPS analysis of the sample of the copper nanowires: (a) Cu 2p; (b) Cu LVV; (c) O 1s.

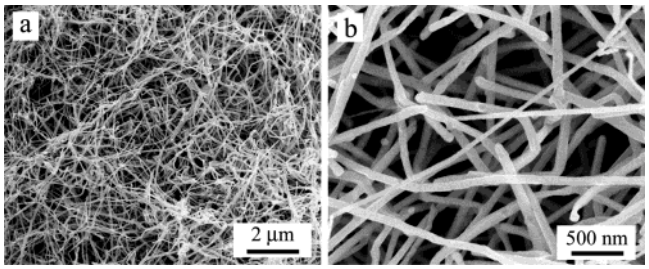

Figure 3. FESEM images of as-obtained copper nanowires: (a) low-magnification view; (b) high-magnification view. The concentrations of $CuSO_4$, glycerol, NaOH, SDBS were 50 mM, 40 vol %, 5 M, and 3 mM, respectively. The reaction temperature was controlled at 120 °C.

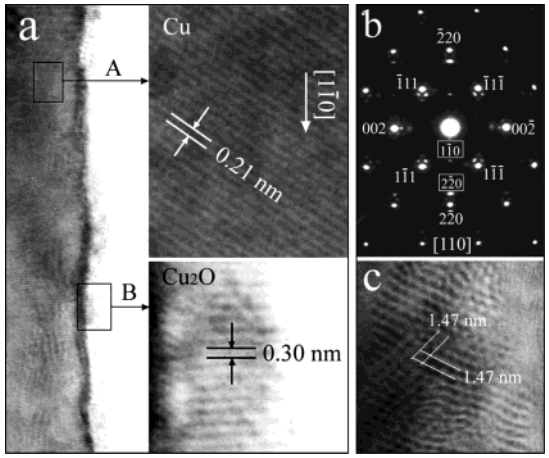

Figure 4. (a) HRTEM image of a copper nanowire. The local enlarged image from the boxed region A and B is also shown in this image. (b) Corresponding SAED pattern, taken along the [110] zone axis perpendicular to the long axis of the nanowire. The diffraction indexes without and with boxes correspond to these of Cu and Cu_2O phase, respectively. The additional diffraction spots along three directions (including [1$\bar{1}\bar{1}$], [1$\bar{1}$1], and [1$\bar{1}$0]) suggest the presence of 7 times superlattice of Cu in the three directions. (c) HRTEM image clearly showing the 7 times superlattice along [1$\bar{1}\bar{1}$] and [1$\bar{1}$1] directions of face-centered cubic Cu.

process. In this mechanism, some small nanoparticles were gradually dissolved to generate free Cu atoms in the solution, and these Cu atoms were spontaneously transferred onto the surfaces of some large crystals with high surface free energies. Obviously, continually adding the copper atoms to the surfaces of these growing rodlike particles at the expense of small nanoparticles should lead to forming the long nanowires. As shown in Figure 5c, the product obtained over 20 h was predominated with uniform nanowires with diameters of ~85 nm. Almost no Cu nanoparticles were observed.

Effect of SDBS on the Nanowires Growth. We found that SDBS was necessary in the present procedure for the synthesis of Cu nanowires. But the exact roles of SDBS on the nanowires

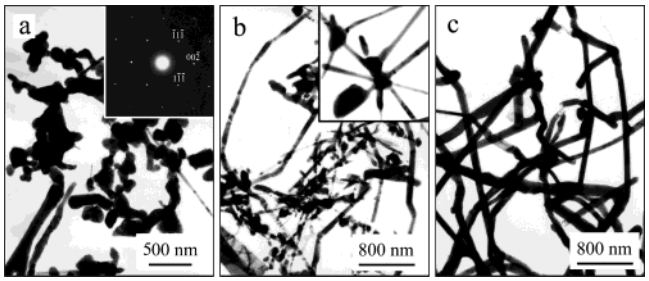

Figure 5. TEM images of three samples, showing different stages of the growth for copper nanowires. These samples were taken after the reaction had been proceeded for (a) 3 h, (b) 10 h, and (c) 20 h, respectively.

growth is still unclear. It could be believed that the surfactant SDBS might play roles on at least two aspects: preventing the aggregation of Cu nanoparticles in the initial stage of nanowire growth and kinetically controlling the growth rates of various crystallographic facets of face-centered cubic Cu through selectively adsorbing on these facets. The roles of SDBS on the formation of Cu nanowires were similar to these of poly(vinylpyrrolidone) (PVP) on the formation of Ag and Pb nanowires.[6] In the absence of SDBS, the reaction only produced very irregular particles with diameters of several hundreds of nanometers, which often appeared as collections of aggregated particles (10 μm in sizes). This indicates that the initial formed copper nanoparticles had a strong tendency to aggregate as larger ones when no protective agents were added. When SDBS was introduced in appropriate amounts, the initially formed nanoparticles were relatively small in dimension, and well dispersed in the solution. We found that Cu nanowires could be produced in high yield at a concentration of SDBS over 2.5 mM. We also found that SDBS was unique for the formation of Cu nanowires in the present synthesis. When other surfactants, such as sodium dodecyl sulfate (SDS), PVP, and cetyltrimethylammonium bromide (CTAB) were used instead of SDBS, no nanowires were produced. The explanation for this probably indicates that they were different in both the carbon chain length and the hydrophilic group, and thus they were alien in modulating the growth kinetics of Cu crystals.

Influences of the Concentrations of NaOH and Glycerol. The concentrations of both NaOH and glycerol in the reaction mixture were two other important factors in determining the morphology of the final product. Though the formation of complex $Cu(C_3H_6O_3)$ needed only a small amount of NaOH and glycerol, the relatively high concentrations of both NaOH solution (~4.5−5.5 M) and glycerol (~40 vol %), which led to forming a mixture with high viscosity, were found to be favorable for the formation of the copper nanowires in high yield. Such a high viscosity had a good effect on prohibiting aggregation of copper particles and then resulted in a relatively stable suspension. Control reactions at a low concentration of NaOH (4 M) or glycerol (25 vol %) would plate out a large

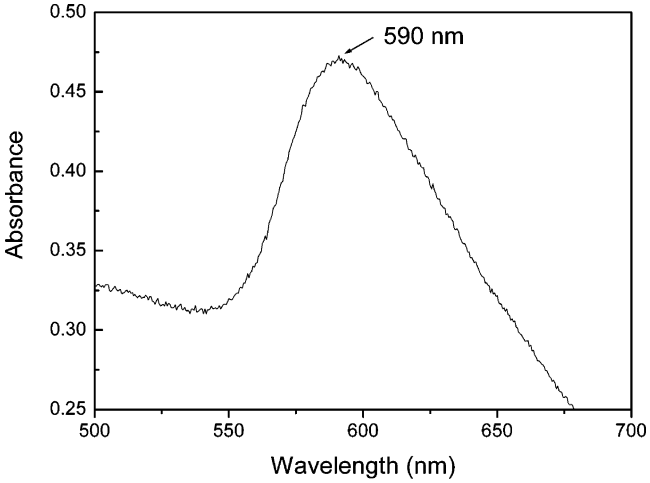

Figure 6. UV−vis spectra of the as-synthesized copper nanowires.

amount of the copper on the sides and bottom of the autoclave. At very high concentrations of NaOH (7 M) and glycerol (55 vol %), however, only the aggregated particles were observed.

Optical Property of Copper Nanowires. Figure 6 shows the UV−vis absorption spectrum taken form the as-synthesized copper nanowires dispersed in ethanol. The adsorption maxima at 590 nm were in good agreement with the reported values for copper nanoparticles,[13] and attributable to the plasma excitation in copper nanowires. This also indicates that the thin oxide layers (mainly Cu_2O phase) on the surfaces of Cu nanowires had little effect on the adsorption edge.

Conclusion

In summary, copper nanowires with a uniform diameter have been successfully prepared in high yield via a complex-surfactant-assisted hydrothermal reduction process at a low temperature. The surfactant SDBS played a crucial role on the copper nanowires growth. The concentrations of NaOH and glycerol also had important effects in determining the morphology of the final product. Because we have also prepared face-centered cubic nickel nanowires and nanoribbons via a method similar to that described in present work, we believe such a rational low-temperature synthetic route is versatile and can be adapted for the fabrication of 1D nanostructures of various transition metals and their alloys by choosing the suitable complexing agents and the reaction parameters.

Acknowledgment. This work was supported by National Natural Science Found of China and the 973 Project of China.

Supporting Information Available: FESEM images of three samples prepared at different concentration of SDBS (PDF) and ED patterns obtained before and after a long-time electron-beam irradiation on a Cu nanowire. This material is available free of charge via the Internet at http://pubs.acs.org.

References and Notes

(1) (a) Hu, J.; T. Odom, W.; Lieber, C. M. *Acc. Chem. Res.* **1999**, *32*, 435. (b) Zhang, Z.; Sun, X.; Dresselhaus, M. S.; Ying, J. Y. *Phys. Rev. B* **2000**, *61*, 4850. (c) Wang, Z. L. *Adv. Mater.* **2000**, *12*, 1295. (d) Sun, L.; Searson, P. C.; Chien, C. L. *Appl. Phys. Lett.* **2001**, *79*, 4429.(e) Cui, Y.; Wei, Q.; Park, H.; Lieber, C. M. *Science* **2001**, *293*, 1298. (f) Gillingham, D. M.; Linington, I.; Bland, J. A. C. *J. Phys.: Condens. Mater.* **2002**, *14*, L567.

(2) Monson, C. F.; Woolley, A. T. *Nano. Lett.* **2003**, *3*, 359.

(3) (a) Chen, P.; Wu, X.; Lin, J.; Tan, K. L. *J. Phys. Chem. B* **1999**, *103*, 4559. (b) Molares, M. E. T.; Brŏtz, J. Bushmann, V.; Dobrev, D.; Neumann, R.; Scholz, R.; Schuchert, I. U.; Trautmann, C. Vetter, J. *Nucl. Instrum. Methods B* **2001**, *185*, 192. (c) Gao, T.; Meng, G.; Wang, Y.; Sun, S.; Zhang, L. *J. Phys.: Condens. Mater.* **2002**, *14*, 355. (d) Hwang, G. L.; Hwang, K. C.; Shieh, Y. T.; Lin, S. J. *Chem. Mater.* **2003**, *15*, 1353. (e) Toimil Molares, M. E.; Hohberger, E. M.; Schaeflein, Ch.; Blick, R. H.; Neumann, R.; Trantmann, C. *Appl. Phys. Lett.* **2003**, *82*, 2193.

(4) (a) Liu, Z. W.; Bando, Y. *Adv. Mater.* **2003**, *15*, 303. (b) Yen, M. Y.; Chiu, C. W.; Hsia, C. H.; Chen, F. R.; Kai, J. J.; Lee, C. Y.; Chiu, H. T. *Adv. Mater.* **2003**, *15*, 235.

(5) (a) Qi, L. M.; Ma, J. M.; Cheng, H. M.; Zhao, Z. G. *J. Phys. Chem. B* **1997**, *101*, 3460. (b) Mayers, B.; Xia, Y. N. *J. Mater. Chem.* **2002**, *12*, 1875. (c) Wang, X.; Li, Y. D. *J. Am. Chem. Soc.* **2002**, *124*, 2880.

(6) (a) Sun, Y. G.; Gates, B.; Mayers, B.; Xia, Y. N. *Nano Lett.* **2002**, *2*, 165. (b) Sun, Y. G.; Yin, Y. D.; Mayers, B.; Herricks, T.; Xia, Y. N. *Chem. Mater.* **2002**, *14*, 4736. (c) Wang, Y. L.; Herricks, T.; Xia, Y. N. *Nano Lett.* **2003**, *3*, 1163.

(7) Wagner, C. D.; Riggs, W. M.; Davis, L. E.; Moulder, J. F. In *Handbook of X-ray Photoelectron Spectroscopy*; Muilenberg, G. E., Ed.; Perkin-Elmer Corp.: Eden Prairie, MN, 1979.

(8) *Practical Surface Analysis by Auger and X-ray Photoelectron Spectroscopy*; Briggs, D.; Seah, M. P., Eds.; John Wiley & Sons: New York, 1983; p 496.

(9) Partain, L. D.; Schneider, R. A.; Donaghey, L. F.; Meleod, P. S. *J. Appl. Phys.* **1985**, *57*, 5056.

(10) Deroubaix, G.; Marcus, P. *Surf. Interface Anal.* **1992**, *18*, 39.

(11) Lisiechi, I.; Filankembo, A.; Sack-Kongehl, H.; Weiss, K.; Pleni, M.-P.; Urban, J. *Phys. Rev. B* **2000**, *61*, 4968.

(12) (a) Onuferko, J. H.; Woodruff, D. P. *Surf. Sci.* **1980**, *95*, 555. (b) Richter, H.; Gerhardt, U. *Phys. Rev. Lett.* **1983**, *51*, 1570. (c) Parkin, S. R.; Zeng, H. C.; Zhou, M. Y.; Mitchell, K. A. R. *Phys. Rev. B* **1990**, *41*, 5432. (d) Robinson, I. K.; Vlieg, E.; Ferrer, S. *Phys. Rev. B* **1990**, *42*, 6954. (e) Durr, H.; Fauster, Th.; Schneider, R. *Surf. Sci.* **1991**, *244*, 237. (f) Kundrotas, P. J.; Lapinskas, S.; Rosengren, A. *Phys. Rev. B* **1997**, *56*, 6486.

(13) Joanna, P.; Cason, M. E.; Thompson, B. J.; Roberts, C. B. *J. Phys. Chem. B* **2001**, *105*, 2297.